AIP Applied Physics Letters

High-performance resistive switching characteristics of programmable metallization cell with oxidized Cu-Ti electrodes

Yu-Chih Huang, Chia-Hsin Chou, Chan-Yu Liao, Wan-Lin Tsai, and Huang-Chung Cheng

Citation: Applied Physics Letters **103**, 142905 (2013); doi: 10.1063/1.4823818
View online: http://dx.doi.org/10.1063/1.4823818
View Table of Contents: http://scitation.aip.org/content/aip/journal/apl/103/14?ver=pdfcov
Published by the AIP Publishing

Articles you may be interested in

Evidence for multifilamentary valence changes in resistive switching SrTiO3 devices detected by transmission X-ray microscopy
APL Mat. **1**, 042102 (2013); 10.1063/1.4822438

Performance and characteristics of double layer porous silicon oxide resistance random access memory
Appl. Phys. Lett. **102**, 253509 (2013); 10.1063/1.4812474

Mechanism of resistive switching in Cu/AlOx/W nonvolatile memory structures
J. Appl. Phys. **113**, 164506 (2013); 10.1063/1.4803062

Effect of oxide insertion layer on resistance switching properties of copper phthalocyanine
AIP Conf. Proc. **1512**, 718 (2013); 10.1063/1.4791239

Texture and resistivity of dilute binary Cu(Al), Cu(In), Cu(Ti), Cu(Nb), Cu(Ir), and Cu(W) alloy thin films
J. Vac. Sci. Technol. B **20**, 2314 (2002); 10.1116/1.1520549

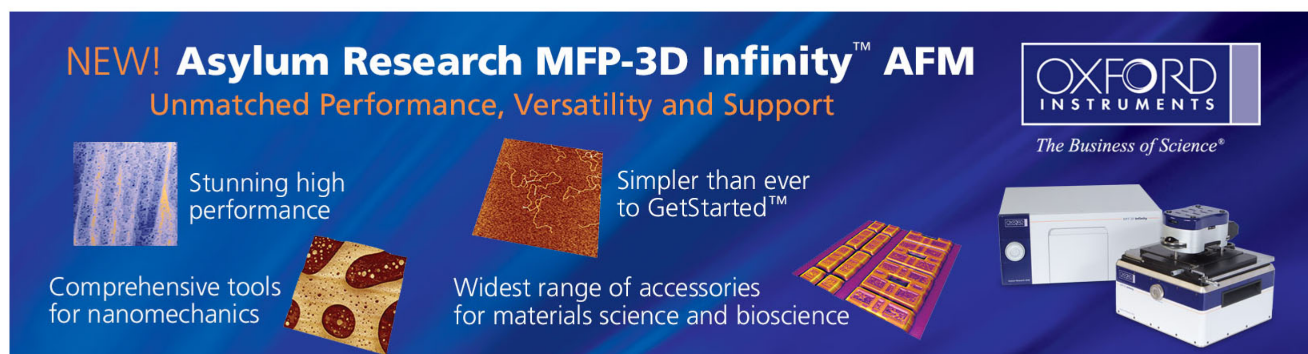

This article is copyrighted as indicated in the article. Reuse of AIP content is subject to the terms at: http://scitation.aip.org/termsconditions. Downloaded to IP: 140.113.38.11 On: Wed, 30 Apr 2014 08:46:32

High-performance resistive switching characteristics of programmable metallization cell with oxidized Cu-Ti electrodes

Yu-Chih Huang, Chia-Hsin Chou, Chan-Yu Liao, Wan-Lin Tsai, and Huang-Chung Cheng
Department of Electronics Engineering and Institute of Electronics, National Chiao Tung University, Hsinchu 30010, Taiwan

(Received 20 August 2013; accepted 14 September 2013; published online 1 October 2013)

Programmable metallization cell (PMC) memory devices with oxidized Cu-Ti alloy films as the bottom electrodes have been shown to exhibit a superior on/off state current ratio (memory window) of as high as 10^3 and endurance of 3000 cycles as compared to conventional pure copper and unoxidized Cu-Ti alloy electrodes. It was conjectured that the Cu-Ti alloy electrodes could obtain the appropriate amount of copper atoms to format and rupture the conductive filaments in the resistive switching layer. Furthermore, the oxidized Cu-Ti alloys could control the Cu cations from the Cu and Cu_2O to the appropriate amountto achieve the most favorable PMC characteristics. © *2013 AIP Publishing LLC*. [http://dx.doi.org/10.1063/1.4823818]

In recent years, resistive random access memory (RRAM) has received significant attention owing to its simple fabrication process, low energy operation, and high stackability for use in the next-generation of nonvolatile memory (NVM) technology.[1] RRAM devices fabricated with electrochemical active metal electrodes, such as Ag or Cu, are also known as programmable metallization cells (PMCs) or conductive bridging RAM (CBRAM).[1–3] The resistive switching phenomena during the set and reset process of the PMC devices is attributed to the formatting and rupturing of the nanoscale metallic conductive filaments (CFs) in the resistive switching layer, respectively.[2–6] During the reset process of the PMC, CFs are ruptured via the reduction-oxidation (redox) process, and most of the metal cations drift to the active electrode. CFs can also be broken and lead to the presence of fragmented metal clusters or atoms in the resistive switching layer.[7–9] An excessive amount of copper atoms in the resistive switching layer can reduce the resistance causing the reset failure of PMCs after a number of resistive switching cycles.[3,10,11] Consequently, many methods have been proposed to limit the amount of metal atoms injected from the active electrode, such as the use of metal compounds as the active electrode,[12–16] adding dissolved metal to the insulating layer,[17,18] and putting metal oxide layers on top of the active electrodes.[19] On the other hand, oxidized Cu in form of CuO makes it more difficult to release the Cu atoms via the redox process than Cu_2O and metallic Cu.[20–23] It is thus feasible that oxidizing copper can limit the release of Cu atoms.

This study proposes using oxidized Cu-Ti alloy oxide films as the bottom electrodes of PMCs in order to limit the injection of copper atoms into the resistive switching layer, resulting in the good reliability through repeated operations, and a large memory window.

First, a 50 nm-thick Pt layer was deposited on the oxidized silicon wafer as the contact metal using a direct-current (DC) sputtering system. Next, a 300 nm-thick Cu-Ti alloy metal layer was deposited on the Pt contact as the bottom electrode with varied Cu:Ti co-sputtering power. Cu-Ti alloys were produced with the following co-sputtering powers of Cu and Ti, 10 W:170 W, 30 W:170 W, and 50 W:170 W, and these are denoted as 10 W Cu-Ti, 30 W Cu-Ti, and 50 W Cu-Ti, accordingly. The samples were subsequently thermal oxidized at 600 °C for 5 min in oxygen ambient with a rapid thermal annealing (RTA) system. The resulting oxidized Cu-Ti specimens are denoted as 10 W Cu-Ti ox, 30 W Cu-Ti ox, and 50 W Cu-Ti ox, respectively. After the oxidation process, a 200 nm-thick TiO_2 layer was reactively sputtered on the bottom electrode as the resistive switching layer, with the Ti target at a power of 190 W, a total pressure of 5×10^{-3} torr, and the flow rates of 22.4 and 9.6 sccm for the Ar and O_2 gases, respectively. Finally, a 50 nm-thick Pt layer was deposited as the disk-shaped top inert electrodes with the diameter of 356.9 μm (area of approximately 100 042 μm^2) through the shadow mask. For comparison purposes, a conventional pure Cu bottom electrode called Pure Cu, and an oxidized pure Cu one denoted as Pure Cu ox were also fabricated. The compositions of the Cu-Ti layers and the chemical bonding states of the Cu-Ti oxide layers were examined with x-ray photoelectron spectroscopy (XPS). The resistive switching characteristics were measured at room temperature in the dark with the unique electrode area by an Agilent 4156 C precision semiconductor parameter analyzer.

The atomic concentrations of Ti and Cu for the as-deposited Cu-Ti alloy layers have been calculated with XPS via the areas of the binding energy peaks of Ti 2p and Cu $2p_3$, as listed in Table I.[13,16] The ratio of Cu to Ti was increased along with the co-sputtering power of Cu. The DC sweep I-V curves of the unoxidized electrode specimens 10 W Cu-Ti, 30 W Cu-Ti, 50 W Cu-Ti, and Pure Cu were started in the reverse bias of 0 V to −4 V for the set process, and then in the forward bias of 0 V to +3 V for the reset process, as shown in Figure 1(a). The current compliance (I_{Comp}) was set at 0.01 A to protect the device from breaking down. A schematic diagram of the I-V measurement is shown in the inset of Figure 1(a). It can be seen that the DC set voltages of 10 W Cu-Ti, 30 W Cu-Ti, 50 W Cu-Ti, and Pure Cu specimens were −1.9 V, −1.7 V, −1.6 V, and −1.5 V, defined by the currents abruptly increased to the compliance valve during the reverse

 © 2013 AIP Publishing LLC

This article is copyrighted as indicated in the article. Reuse of AIP content is subject to the terms at: http://scitation.aip.org/termsconditions. Downloaded to IP: 140.113.38.11 On: Wed, 30 Apr 2014 08:46:32

TABLE I. The compositions of the Cu and Ti atoms in atomic ratios for the as-deposited Cu-Ti alloys at different co-sputtering powers for the Cu components and the pure Cu specimen based on the ratios of the XPS peak areas corresponding to Cu $2p_3$ and Ti 2p.

Composition	10 W Cu-Ti	30 W Cu-Ti	50 W Cu-Ti	Pure Cu
Cu $2p_3$	36%	41%	52%	100%
Ti 2p	64%	59%	48%	0%

DC bias sweep, respectively. In order to fairly compare the repeated reliability, the operating parameters with the set/reset pulse voltages of −8 V/+3 V for setting/resetting process, the read voltage of 0.1 V for reading the ON-state/OFF-state currents, with the pulse width of 1 μs, and the I_{Comp} of 0.01 A were applied for all the samples. The endurance measurements were performed after the DC bias sweep measurements for the same sample and according to the following sequences of operating cycle: setting, reading for ON-state current, resetting, reading for OFF-state current, and back to setting. The repeated resistive switching characteristics for the 10 W Cu-Ti samples were exhibited 1000 endurance cycles with an initial on/off current ratio (memory window) of 2.3 orders, 800 endurance cycles and 2.2 orders for the 30 W Cu-Ti ones, 600 endurance cycles and 2.1 orders for the 50 W Cu-Ti ones, and 400 endurance cycles and 1.7 orders for the Pure Cu ones, as shown in Figure 1(b). For the unoxidized electrode specimens, the DC set voltages, endurances, and on/off currents were negatively related to the Cu compositions for the pure Cu and Cu-Ti alloys, as seen in Figures 1(a) and 1(b), and listed in Table I. It was conjectured that the increased Cu cations of the electrodes would diffuse and drift into the TiO_2 resistive switching layers, and thus the driving electrical fields needed to format the CFs could be reduced, lowering the DC set voltages. On the other hand, the excessive amount of Cu atoms residing in the TiO_2 resistive switching layers after the reset process would increase the off state currents and the reset failure probability, thus resulting in shorter resistive switching cycles and the lower memory windows than seen with a lower Cu composition.

As for the oxidized electrode samples, the DC sweep I-V curves of the 10 W Cu-Ti ox, 30 W Cu-Ti ox, 50 W Cu-Ti ox, and Pure Cu ox were obtained with the same measurement parameters as the unoxidized electrode ones, as shown in Figure 2(a). It can be seen that all the 30 W Cu-Ti ox, 50 W Cu-Ti ox, and Pure Cu ox specimens had resistive switching properties, except the 10 W Cu-Ti ox ones. The DC set voltages of 30 W Cu-Ti ox, 50 W Cu-Ti ox, and Pure Cu ox samples were −2.2 V, −1.6 V, and −3.5 V, respectively. The repeated resistive switching characteristics for the 30 W Cu-Ti ox specimens achieved 3000 endurance cycles with the initial memory window of 3.8 orders, 800 endurance cycles and 3 orders for the 50 W Cu-Ti ox ones, and 1000 endurance cycles and 3 orders for the Pure Cu ox ones, as shown in Figure 2(b). The 30 W Cu-Ti ox samples obviously had the best repeated resistive switching characteristics, including the greatest endurance and the largest memory window of all these specimens. In order to better understand the significant differences among the resistive switching characteristics for the oxidized pure Cu and Cu-Ti samples, the chemical bonding states of the Cu elements of the oxidized electrodes, including the Cu-Ti 10 W ox, Cu-Ti 30 W ox, Cu-Ti 50 W ox, and Pure Cu ox ones, were analyzed based on the XPS data, as shown in Figures 3(a)–3(d), respectively. The XPS results for the Cu $2p_3$ core level can be divided into three sub-peaks approximately centered at 932.2 eV, 932.7 eV, and 933.8 eV by Gaussian fitting, respectively, for the metallic Cu, the copper ions (cations) with the oxidation state of Cu^+ (Cu_2O), and the copper cations with the oxidation state of Cu^{2+} (CuO). In addition, the XPS results for the Ti 2p core level can also be divided into three sub-peaks approximately centered at 460.1 eV, 462.0 eV, and 464.7 eV, respectively, for the metallic Ti, Ti^{3+} (Ti_2O_3), and Ti^{4+} (TiO_2). The proportions of these sub-peaks can be calculated from the peak areas.[16] The compositions of the metallic Cu, Cu^+, Cu^{2+}, metallic Ti, Ti^{3+}, and Ti^{4+} for the oxidized Cu-Ti alloy and oxidized pure Cu were assessed, and these are listed in Table II.

According to previous reports,[20–23] Cu_2O can release Cu atoms via the redox process, which can be described with the following reaction equation:

$$Cu_2O \rightarrow CuO + Cu. \quad (1)$$

Therefore, both the metallic Cu and Cu_2O could contribute the majority of the Cu cations to format the CFs for the oxidized Cu-Ti alloys and oxidized pure Cu electrodes. In contrast, CuO is the higher oxide of copper, and thus the Cu atoms have stronger bonds to the oxygen atoms, making it more difficult to release the Cu cations in comparison to the metallic Cu and Cu_2O. On the other hand, the metallic Ti and Ti oxides (Ti_2O_3 and TiO_2) are not the chemically active metal sources, and thus cannot format the CFs. Consequently,

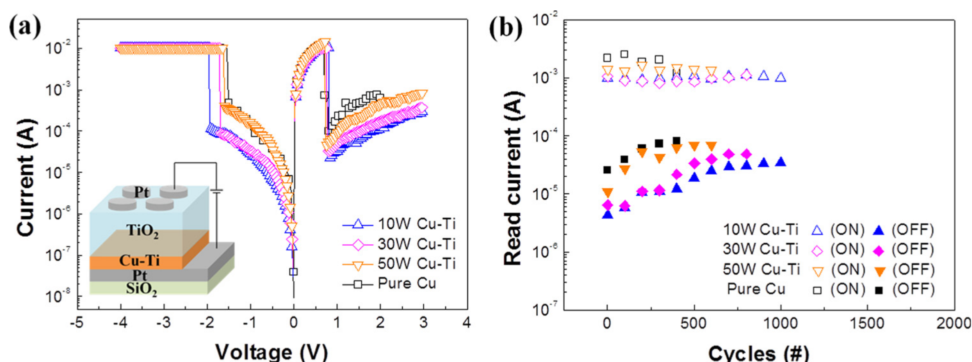

FIG. 1. (a) The DC sweep I-V curves and structure diagrams of the unoxidized electrode specimens. (b) Endurances of the unoxidized electrode specimens.

This article is copyrighted as indicated in the article. Reuse of AIP content is subject to the terms at: http://scitation.aip.org/termsconditions. Downloaded to IP: 140.113.38.11 On: Wed, 30 Apr 2014 08:46:32

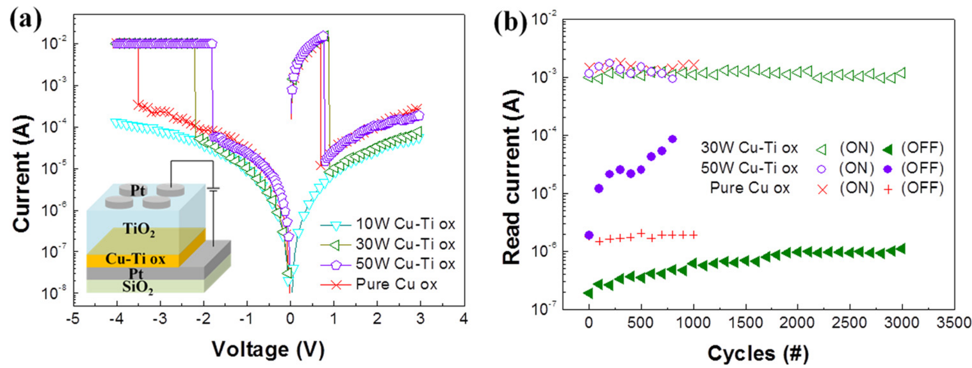

FIG. 2. (a) The DC sweep I-V curves and structure diagrams of the oxidized electrode samples. (b) Endurances of the oxidized electrode samples.

as demonstrated in Table II and Figures 2(a) and 2(b), the 10 W Cu-Ti ox samples had the least Cu and Cu_2O contents among all the oxidized Cu and Cu-Ti alloy samples, and thus exhibited no resistive switching property. In contrast, the 50 W Cu-Ti ox ones possessed the highest Cu and Cu_2O contents, and thus it is easier to format the CFs using these during the set process, with the lowest DC set voltage, although these are also more likely to lead to Cu atoms being present in the TiO_2 resistive switching layer during the reset process, resulting in the smallest final memory window and the worst endurance among all the oxidized specimens examined in this work. On the other hand, the Pure Cu ox ones have the second most Cu and Cu_2O contents, with a moderate final memory window and endurance. As for the 30 W Cu-Ti ox ones, they had the most appropriate amount of the Cu and Cu_2O, and thus the greatest final memory window and endurance. Since it is difficult for CuO to release the Cu cations needed to format the CFs, and the Pure Cu ox specimen has the most CuO, it also has the largest DC set voltage among all the oxidized electrodes. It is worth noting that the 30 W Cu-Ti ox specimens could obtain the appropriate quantity of Cu cations from the metallic Cu and Cu_2O, and thus have excellent set and reset properties. As compared to the unoxidized Cu-Ti and pure Cu electrodes, the oxidized ones could significantly reduce the amount of Cu cations released from the metallic Cu and Cu_2O, thus improving the memory window and endurance.

In summary, high-performance PMC devices with oxidized 30 W Cu-Ti alloys as the active electrodes have been demonstrated to achieve a memory window of 3.8 orders and endurance as long as 3000 cycles, as compared to 1.6 orders and 400 cycles for the conventional pure Cu electrode samples, and 2.3 orders and 1000 cycles for the unoxidized 10 W Cu-Ti ones. It was conjectured that the oxidized Cu-Ti alloys

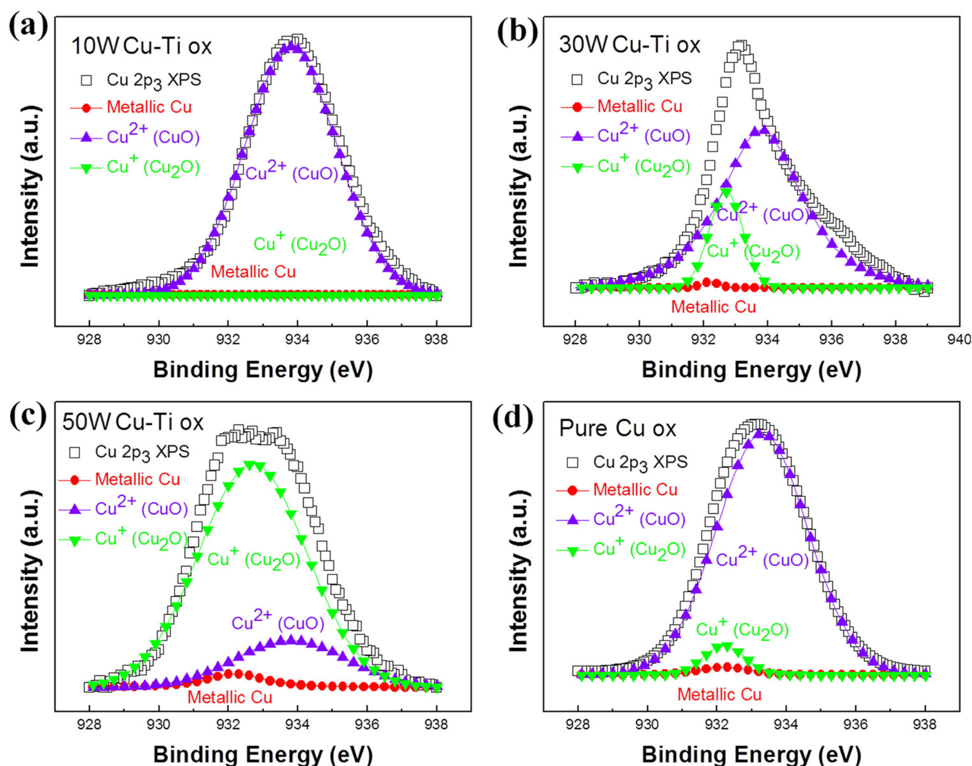

FIG. 3. XPS data of the Cu $2p_3$ core level divided into three peaks (Metallic Cu, Cu^{2+}, and Cu^{+}) by Gaussian fitting for the sample of (a) 10 W Cu-Ti ox, (b) 30 W Cu-Ti ox, (c)50 W Cu-Ti ox, and (d) Pure Cu ox.

This article is copyrighted as indicated in the article. Reuse of AIP content is subject to the terms at: http://scitation.aip.org/termsconditions. Downloaded to IP: 140.113.38.11 On: Wed, 30 Apr 2014 08:46:32

TABLE II. The compositions of the metallic Cu, Cu^{2+}, Cu^{+}, metallic Ti, Ti^{4+}, and Ti^{3+} in atomic ratios for the oxidized Cu-Ti alloys at different co-sputtering powers for the Cu components and the oxidized pure Cu specimen based on the ratios of the XPS sub-peak areas corresponding to Cu $2p_3$ and Ti 2p.

Bonding states	10 W Cu-Ti ox	30 W Cu-Ti ox	50 W Cu-Ti ox	Pure Cu ox
Metallic Cu	0.4%	0.8%	3.6%	4.0%
Cu^{2+} (CuO)	35.2%	34.9%	8.9%	90.0%
Cu^{+} (Cu_2O)	0.4%	5.3%	39.5%	6.0%
Metallic Ti	1.2%	0.6%	0.2%	0%
Ti^{4+} (TiO_2)	60.7%	56.9%	47.2%	0%
Ti^{3+} (Ti_2O_3)	2.1%	1.5%	0.6%	0%

could significantly control the release of Cu cations from the metallic Cu and Cu_2O by achieving an appropriate amount for formatting and rupturing the CFs in the resistive switching layers. PMCs with oxidized Cu-Ti alloys as the active electrodes are thus promising for the next-generation of non-volatile memory devices.

The authors at NCTU thank the National Science Council of Taiwan under Contract No. NSC 101-2221-E-009-077-MY3. The authors would like to thank the Nano Facility Center (NFC) of National Chiao Tung University and the National Nano Device Laboratories (NDL) for technical supports.

[1]R. Waser, R. Dittmann, G. Staikov, and K. Szot, Adv. Mater. **21**, 2632 (2009).
[2]U. Russo, D. Kamalanathan, D. Ielmini, A. L. Lacaita, and M. N. Kozicki, IEEE Trans. Electron Devices **56**, 1040 (2009).
[3]S. Yu and H. -S. P. Wong, IEEE Trans. Electron Devices **58**, 1352 (2011).
[4]J. Billen, S. Steudel, R. Müller, J. Genoe, and P. Heremans, Appl. Phys. Lett. **91**, 263507-1 (2007).
[5]N. Banno, T. Sakamoto, N. Iguchi, H. Sunamura, K. Terabe, T. Hasegawa, and M. Aono, IEEE Trans. Electron Devices **55**, 3283 (2008).
[6]T. Tsuruoka, K. Terabe, T. Hasegawa, and M. Aono, Nanotechnology **21**, 425205-1 (2010).
[7]D. Yu, L. F. Liu, P. Huang, F. F. Zhang, B. Chen, B. Gao, Y. Hou, D. D. Han, Y. Wang, J. F. Kang, and X. Zhang, in Proceedings of the IEEE Silicon Nanoelectronics Workshop, 2012.
[8]N. Banno, T. Sakamoto, S. Fujieda, and M. Aono, IEEE Int. Reliab. Phys. Symp. Proc. **2008**, 707.
[9]A. Vena, E. Perret, S. Tedjini, C. Vallée, P. Gonon, and C. Mannequin, IEEE MTT-S Int. Microwave Symp. Dig. **2012**, 1.
[10]L. Zhang, R. Huang, D. Gao, D. Wu, Y. Kuang, P. Tang, W. Ding, A. Z. H. Wang, and Y. Wang, IEEE Electron Device Lett. **30**, 870 (2009).
[11]H. Xie, Q. Liu, Y. Li, H. Lv, M. Wang, K. Zhang, S. Long, S. Liu, and M. Liu, Semicond. Sci. Technol. **27**, 105007-1 (2012).
[12]L. Goux, K. Sankaran, G. Kar, N. Jossart, K. Opsomer, R. Degraeve, G. Pourtois, G. M. Rignanese, C. Detavernier, S. Clima, Y. Y. Chen, A. Fantini, B. Govoreanu, D. J. Wouters, M. Jurczak, L. Altimime, and J. A. Kittl, Dig. Tech. Pap.-Symp. VLSI Technol. **2012**, 69.
[13]M. N. Kozicki, C. Gopalan, M. Balakrishnan, and M. Mitkova, IEEE Trans. Nanotechnol. **5**, 535 (2006).
[14]K. Aratani, K. Ohba, T. Mizuguchi, S. Yasuda, T. Shiimoto, T. Tsushima, T. Sone, K. Endo, A. Kouchiyama, S. Sasaki, A. Maesaka, N. Yamada, and H. Narisawa, IEEE Tech. Dig. - Int. Electron Devices Meet. **2007**, 783.
[15]L. Goux, K. Opsomer, R. Degraeve, R. Muller, C. Detavernier, D. J. Wouters, M. Jurczak, L. Altimime, and J. A. Kittl, Appl. Phys. Lett. **99**, 053502 (2011).
[16]L. W. Feng, C. Y. Chang, Y. F. Chang, W. R. Chen, S. Y. Wang, P. W. Chiang, and T. C. Chang, Appl. Phys. Lett. **96**, 052111-1 (2010).
[17]J. Park, W. Lee, M. Choe, S. Jung, M. Son, S. Kim, S. Park, J. Shin, D. Lee, M. Siddik, J. Woo, G. Choi, E. Cha, T. Lee, and H. Hwang, IEEE Tech. Dig. - Int. Electron Devices Meet. **2011**, 3.7.1.
[18]Y. S. Chen, H. Y. Lee, P. S. Chen, K. H. Tsai, T. Y. Wu, W. S. Chen, C. H. Tsai, P. Y. Gu, Y. Y. Liao, F. Chen, C. H. Lien, and M. J. Tsai, in *Proceedings of the International Symposium on VLSI-Technology, Systems, and Applications* (VLSI-TSA) (IEEE, 2012), p. 1.
[19]H. J. Wan, P. Zhou, L. Ye, Y. Y. Lin, J. G. Wu, H. Wu, and M. H. Chi, J. Vac. Sci. Technol. B **27**, 2468 (2009).
[20]A. Soon, M. Todorova, B. Delley, and C. Stampfl, Surf. Sci. **601**, 5809 (2007).
[21]C. H. Xua, C. H. Woo, and S. Q. Shi, Superlattices Microstruct. **36**, 31 (2004).
[22]K. Nagase, Y. Zheng, Y. Kodama, and J. Kakuta, J. Catal. **187**, 123 (1999).
[23]A. O. Musa, T. Akomolafe, and M. J. Carter, Sol. Energy Mater. Sol. Cells **51**, 305 (1998).

This article is copyrighted as indicated in the article. Reuse of AIP content is subject to the terms at: http://scitation.aip.org/termsconditions. Downloaded to IP: 140.113.38.11 On: Wed, 30 Apr 2014 08:46:32